

The effects of grain-scale properties on the rapid compaction of sand

Cite as: AIP Conference Proceedings **2272**, 110009 (2020); <https://doi.org/10.1063/12.0000938>
Published Online: 04 November 2020

J. I. Perry, C. H. Braithwaite, N. E. Taylor, and A. P. Jardine



View Online



Export Citation

ARTICLES YOU MAY BE INTERESTED IN

[Material effects on the spallation response of metals and alloys](#)

AIP Conference Proceedings **2272**, 120017 (2020); <https://doi.org/10.1063/12.0000802>

[Effect of texture on elastic precursor decay in magnesium alloy AZ31B](#)

AIP Conference Proceedings **2272**, 120009 (2020); <https://doi.org/10.1063/12.0000818>

[Shock structure and spall behavior of porous aluminum](#)

AIP Conference Proceedings **2272**, 120015 (2020); <https://doi.org/10.1063/12.0000913>



Your Qubits. Measured.

Meet the next generation of quantum analyzers

- Readout for up to 64 qubits
- Operation at up to 8.5 GHz, mixer-calibration-free
- Signal optimization with minimal latency

Find out more



The Effects of Grain-Scale Properties on the Rapid Compaction of Sand

J. I. Perry^{1, a)}, C. H. Braithwaite¹, N. E. Taylor¹ and A. P. Jardine¹

¹*SMF Group, Cavendish Laboratory, University of Cambridge, Cambridge, UK*

^{a)}*Corresponding author: jip24@cantab.net*

Abstract. We review recent experimental efforts at the Cavendish Laboratory regarding the dynamic response of silica sand under a variety of loading rates and geometries – principally plate impact and ballistic penetration. By studying the response of several similar sands in multiple loading scenarios, significant insight has been gained into the key phenomena controlling response. While dynamic behavior is largely controlled by grain-grain contact phenomena, there is a shift from shear behavior and lubrication dominating low rates (where long-range force chains dominate), to compression and stress focusing at high rates – with the transition occurring around the sound speed of the granular material in question.

INTRODUCTION

Understanding the dynamics of granular materials is critical for many applications, from manufacturing processes to asteroid impacts. However, their inherent complexity means that a complete theoretical description remains a substantial challenge [1]. Experimental studies therefore remain extremely important, although variations in materials and methods employed in the literature make comparisons and collation difficult. Experimental data comparing different morphologies and moisture content in particular is lacking, limiting the extent to which one can extrapolate models to predict the dynamic properties of any new granular material of interest.

Two primary experimental techniques have been employed here – Hugoniot determination via planar shock loading, and direct measurement of displacement within a cylindrical granular target during ballistic penetration at 320 ms^{-1} – to study three similar sands under dry and wetted conditions, in order to better understand the effect of grain-scale properties and loading conditions on compaction behavior. This paper collates results from four recent journal articles [2-5], each of which provides detailed methods for the experiments outlined here. While each article has provided insight into one particular aspect of the rapid dynamic response of sand, by combining the results a more comprehensive understanding of the influence of grain-scale properties on rate dependence can be revealed.

MATERIALS

Three similar silica sands have been studied in the experiments presented here. The ‘rough sand’ is a light brown-orange, uniform, fine builders’ sand; the ‘smooth sand’, Leighton Buzzard Fraction D (sourced from David Ball Group, UK), has translucent white grains and a more weathered grain surface; the ‘sandy loam’ is very similar to the rough sand except for the presence of silt (c.10%_{wt}) and a small organic component (c.1-2%_{wt}). The smooth sand is 99.8%_{wt} quartz, while the rough sand contains 6-7%_{wt} orthoclase, and the sandy loam 2-3%_{wt} orthoclase and 1.6-2%_{wt} goethite. All materials were sieved at $850 \mu\text{m}$ to remove a small number of large grains, then dried for 24 h at $120 \text{ }^\circ\text{C}$ to remove residual moisture. Microscope images of the three sands are given in Figure 1, and particle size distributions (as measured with a Malvern Mastersizer 2000) are shown in Figure 2(a).

The density of granular materials is highly dependent on grain morphology, sample geometry and filling conditions. Therefore, some variation in initial density between materials was necessary to ensure samples were stable to additional vibration, did not contain large internal voids, and were not significantly pre-compressed. Under dry

conditions, plate impact sample densities were $(1.38-1.45) \text{ g cm}^{-3}$ for rough sand, $(1.58-1.61) \text{ g cm}^{-3}$ for smooth sand, and $(1.43-1.49) \text{ g cm}^{-3}$ for sandy loam. The much larger ballistic penetration samples had densities of $(1.49-1.51) \text{ g cm}^{-3}$ for rough sand and sandy loam, and $(1.51-1.53) \text{ g cm}^{-3}$ for smooth sand. For moist samples, sand and water were mixed in suitable quantities in a 3-axis turbulent powder mixer before being placed into the experimental targets. Wetted samples have an additional complication in that distention of the granular structure from liquid bridges ('bulking of sand') slightly decreases the density of the solid (granular) phase. For plate impact cells, the 10% moist rough and smooth sand was lightly manually compacted in the cells to $(1.60-1.64) \text{ g cm}^{-3}$, $(1.45-1.49) \text{ g cm}^{-3}$ of which was solid material. For penetration experiments on moist rough sand, densities were $(1.44-1.46) \text{ g cm}^{-3}$ at 2% moisture and $(1.55-1.57) \text{ g cm}^{-3}$ at 10% moisture, of which 1.42 g cm^{-3} was solid material. Moisture content is defined as mass of water/mass of dry sand.

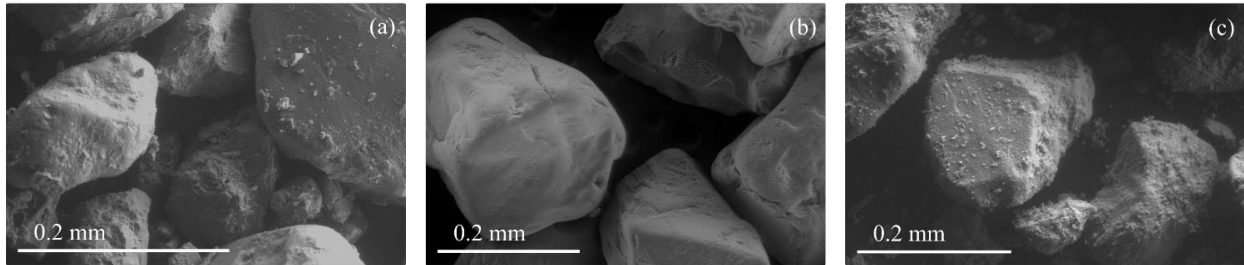


FIGURE 1. ESEM and optical images of the three sands used: (a) rough sand, (b) smooth sand and (c) sandy loam. While the grains are similarly shaped, the grain surfaces on the smooth sand are substantially more weathered, and the sandy loam contains a number of smaller particles. Reprinted (adjusted) with permission from Appl. Phys. Lett. 109, 174103 (2016). Copyright 2016 American Institute of Physics.

QUASI-STATIC COMPACTION

Quasi-static (QS) compaction experiments were performed on the three materials in a gauged reactive (GREAC) cell [6], between 10 mm diameter high strength steel punches and radially confined by a maraging steel annulus at 0.02 mm s^{-1} , using a method similar to Neal et al [7]. Results [4] are given in Figure 2 (b). Little difference is observed between the rough sand and sandy loam, indicating that at low rate the presence of a small silt fraction does not affect compaction. The smooth sand, however, is substantially more resistant to compaction, and (as illustrated in greater detail in [4]) exhibits an initially stiffer region before the granular skeleton yields at approximately 20 MPa. This feature is not present for the other two materials, where breakage of loose asperities enables grain rearrangement to commence at negligible stresses.

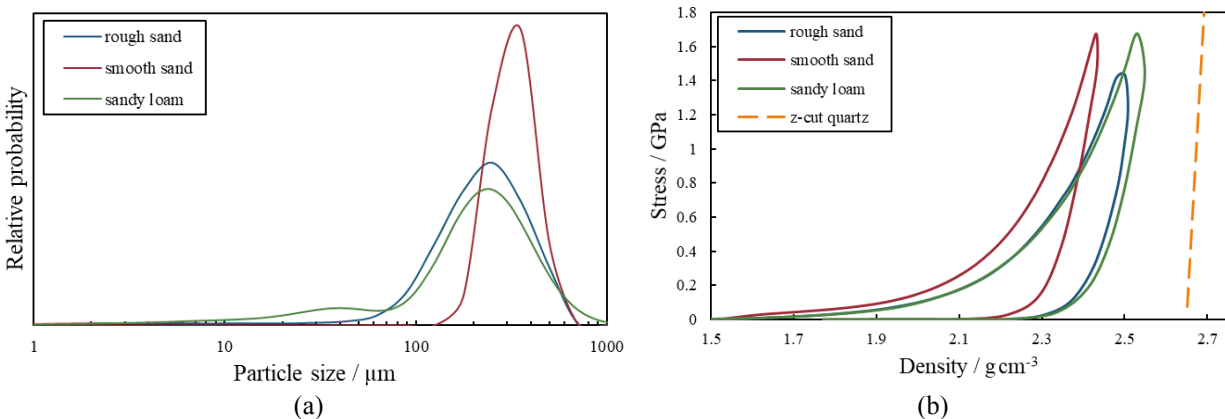


FIGURE 2. (a) Particle size distribution for the three sands studied, and (b) QS compaction data for the two materials in a GREAC cell. Reprinted with permission from Appl. Phys. Lett. 109, 174103 (2016). Copyright 2016 American Institute of Physics.

PLATE IMPACT

One-dimensional plate impact experiments were performed using the 2 inch bore Cavendish Plate Impact Facility light gas gun [8]. The 4 mm deep cylindrical sand samples, fronted with PMMA and backed with a thin copper shim, were impacted with PMMA or copper flyer plates; a thin copper make-trigger (consisting of two strips of copper adhered to the target being shorted together by the conducting flyer plate) and Photon Doppler Velocimetry (PDV) measured shock arrival at the front and rear of the target respectively. Time-of-flight and impedance matching techniques were employed to determine shock velocity, particle velocity and stress in the sand bed; details of the full method have been published previously [2, 3].

Under dry conditions, the three sands' Hugoniot differ from one another by a statistically significant margin, as discussed previously [4, 9]. The sandy loam has a notably lower impedance, while the smooth sand has a shock velocity which varies less with particle velocity – having a similar shock velocity to rough sand at particle velocities of about 500 ms^{-1} . The shock impedance of rough sand is reduced by addition of a small amount of moisture, likely due to lubrication of grain-grain contacts facilitating compaction and water (having a lower sound speed than quartz) slowing the overall shock. For the smooth sand, where dry inter-grain friction is lower, addition of moisture does not markedly decrease impedance but rather aligns it with that of moist rough sand. These results reinforce the argument that grain-grain contact points strongly influence shock velocity, such that when the contacts are wetted, the effects of grain surface roughness are reduced.

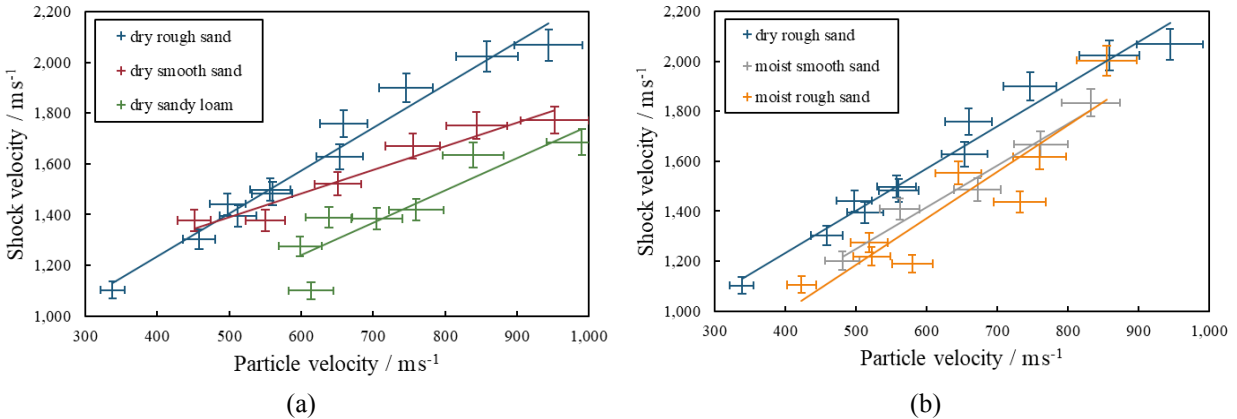


FIGURE 3. (a) The Hugoniot of all three dry sands, showing significant divergence despite having very similar density, morphology and mineralogy. (b) Hugoniot for dry and moist rough sand compared with moist smooth sand. Note how the two materials exhibit similar Hugoniot when wetted. Reprinted with permission from AIP Conference Proceedings 1979, 110002 (2018). Copyright 2018 American Institute of Physics.

BALLISTIC PENETRATION

Here, 150 mm long cylindrical sand targets, 100 mm in diameter, were impacted normally, end-on by 10 mm steel ball bearings at $322 \pm 5 \text{ ms}^{-1}$ using the Cavendish single-stage light gas gun. The experimental procedure [10, 11] was enhanced for use with both dry and moist sand [5]. The targets were contained radially within a polycarbonate cell and at each end with a sheet of card and thin plastic film; a thin copper make-trigger recorded impact timing. Digital Speckle Radiography (DSR) was used to track granular flow during impact [12], imaging a random speckle pattern of lead grains in the horizontal impact plane both before and at a set time after impact. Digital Image Correlation was employed to determine motion of the bed between the two images.

Each experiment provides a single ‘snapshot’ of penetration depth at a specific time following impact, and so each curve in Figure 4 consists of data collated from multiple similar experiments with varying time delay (a) and moisture content (b). For the dry materials, the rough sand and sandy loam exhibit very similar resistance to penetration, while the smooth sand is markedly better at stopping the projectile. The addition of moisture significantly decreases the sand bed’s stopping power, however, with the greatest difference occurring by just c.2% moisture – when the number of liquid bridges is expected to be maximal [13].

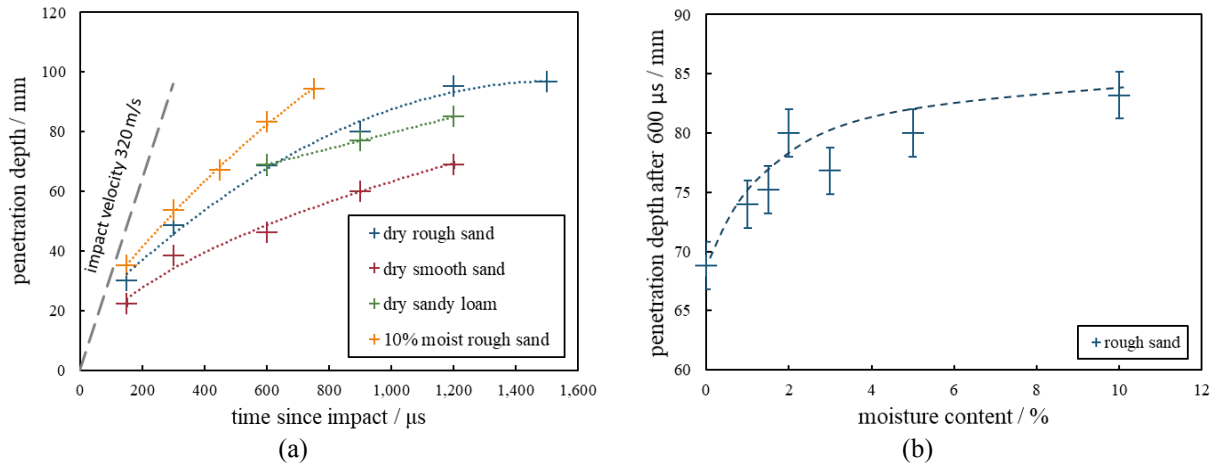


FIGURE 4. (a) Penetration depth as a function of time into the three dry sands and 10% moist ‘rough’ sand, showing how resistance to penetration can vary markedly between the materials despite very similar bulk properties. (b) Penetration depth after 600 μs as a function of moisture content for the rough sand. Curve is illustrative only. Reprinted (adjusted) with permission from Appl. Phys. Lett. 115, 084102 (2019). Copyright 2019 American Institute of Physics.

Further insight can be gained by considering the flow fields as determined by DSR, a selection of which are presented in Figure 5. As the projectile progresses through the sand bed, a compaction wave develops away from the projectile both ahead and laterally. While the dry rough sand and sandy loam exhibit almost identical flow fields, in the moist sample the projectile appears to slip through the target with much less compaction both longitudinally and radially. Conversely in the dry smooth sand, after 600 μs there is significant compaction in the sand bed at twice the depth of the penetrator. Taken together, these flow fields highlight how penetration resistance in brittle granular media is largely controlled by the volume of material set in motion by the penetrator.

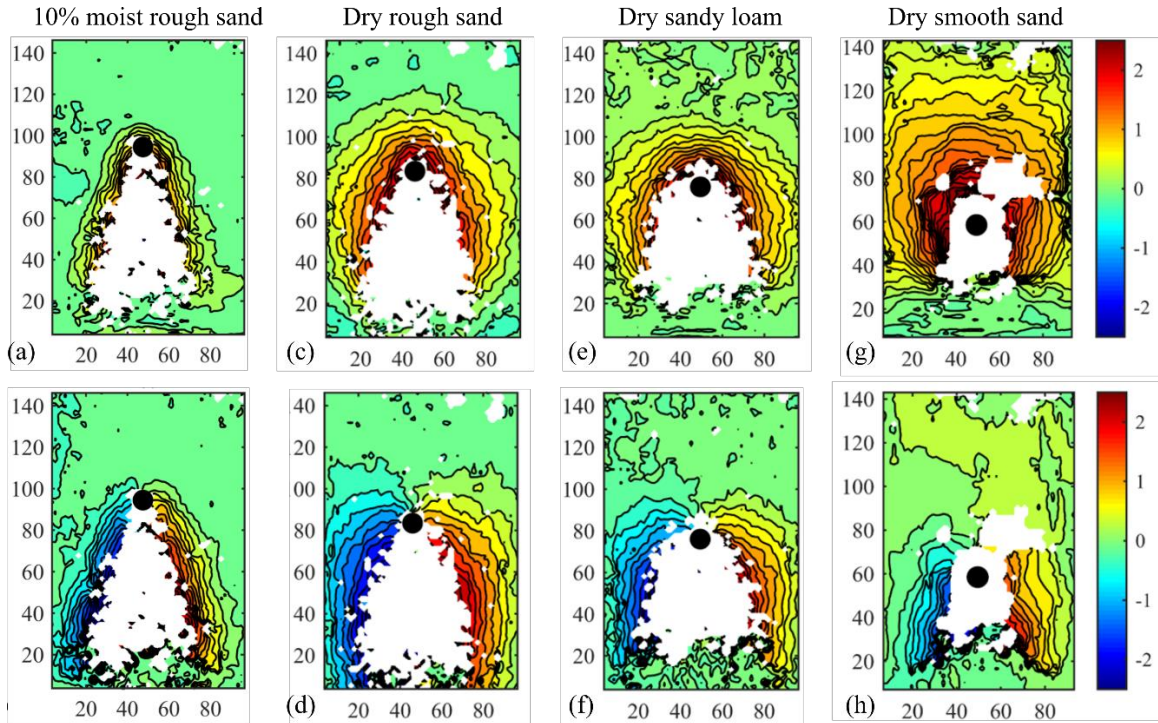


FIGURE 5. Longitudinal (top) and lateral (bottom) flow field diagrams, indicating displacement 750 μs (moist sand) and 900 μs (three dry sands) after impact at 320 m s^{-1} (upwards from below in the images). All values are in mm; the black circles denote projectile location. Areas of white correspond to insufficient correlation, not necessarily due to a void.

Given that the materials studied have very similar bulk properties, the origin of this variation in response must lie at the grain scale. Propagation of a compaction wave away from the projectile requires transmission of stress from grain to grain, in long-range ‘force chains’. In the moist sand, reduction in shear strength due to grain lubrication reduces the ability of these force chains to ‘lock up’, and indeed more readily allows for bulk flow within the target – and so wetted sand offers less penetration resistance. Conversely, the compaction resistance of the smooth sand enhances lock-up behavior and thus increases stopping power.

DISCUSSION

At low rate, compaction is controlled by grain morphology and surface texture – notably the shear response of grain-grain contacts. Smoother grains can more easily re-configure the granular skeleton to spread the load stress more effectively across all grains via long-range force chains, resulting in a more rigid response. This process is inhibited in rougher sands, where instead attrition and abrasion of loose asperities at low stresses creates fines, and certain grains are preferentially loaded to very high stresses, enhancing fracture. For the ballistic impact experiments, penetration resistance depends on the volume of sand to which momentum is transferred from the projectile, which is controlled by the extent to which long-range force chains can propagate stresses away from the projectile. The majority of the resulting deformation occurs some distance away from the projectile, at sub-sonic rates in the sand bed, and results suggest QS compaction behavior and ballistic stopping power are strongly correlated for the impact velocities studied here. At very high rates, grain rearrangement and force-chain creation is suppressed and morphological differences have less effect. Instead, the compaction wave is dominated by the (compressive) coupling of shock-waves across contact points, which can be modified by the presence of either moisture or fines.

The results have begun to show how particular features of a granular bed affect dynamic response in a rate-dependent fashion. Fines appear to make little difference below shock speeds, while smoother grains can either increase or decrease resistance to compaction depending on rate. If one were to project the Hugoniot in Figure 3(a) backwards linearly to zero particle velocity, the impedance of the sandy loam and rough sand are likely similar, while the smooth sand would be much stiffer. Although such a projection should be considered cautiously, it would corroborate with the QS compaction data. Notably, while the literature often discusses ‘critical velocities’ above and below which different penetration equations hold, the reality is likely both more complex and less well-defined. Comparing the rough and smooth dry sand, for example, the different Hugoniot gradients illustrate an inversion from the smooth being stiffer at low rate to the rough at high rate – the apparent cut-off simply arising from differences in Hugoniot gradients rather than any distinct change in response associated with a particular velocity.

To conclude, it has been shown that materials whose granular properties differ only in relatively minor ways, such as the presence of a small silt component or smoother grain surfaces, can exhibit significant variation in dynamic compaction response. Secondly, the disparity in response due to these grain-scale properties may manifest differently depending on the conditions under which they are loaded – principally moisture, rate and geometry. The insights presented here offer a significant advantage to the modelling community with respect to developing accurate morphology- and rate-sensitive material models. However, silica sands include a massive variety of naturally occurring granular materials, from highly angular lunar regolith through to rounded dune sands and glassy volcanic spherules. The interplay between microscopic surface roughness, larger-scale angularity, grain size and shape distribution are complex, and a more complete understanding of these materials will require extensive experimentation across a wider range of materials in the future.

ACKNOWLEDGMENTS

This research was supported through a DSTL Force Protection Engineering research programme led by QinetiQ plc. We thank the staff of the Cavendish Laboratory Workshops for technical assistance and P. Gould and P. Church of QinetiQ for their interest and modelling support.

REFERENCES

1. Blumenfeld, R., S.F. Edwards, and S.M. Walley, *Physics of granular systems - where to go from here*, in *The Oxford handbook of soft condensed matter*, E.M. Terentjev and D.A. Weitz, Editors. 2015, Oxford University Press: Oxford. p. 167.
2. Braithwaite, C.H., et al., *Applied Physics Letters*, 2013. **103**: p. 154103.

3. Perry, J.I., et al., [Applied Physics Letters](#), 2015. **107**: p. 174102.
4. Perry, J.I., et al., [Applied Physics Letters](#), 2016. **109**(17): p. 174103.
5. Perry, J.I., et al., [Applied Physics Letters](#), 2019. **115**(8): p. 084102.
6. Sheridan, A.J. and A.D. Pullen, [Magazine of Concrete Research](#), 2014. **66**(1): p. 50-59.
7. Neal, W.D., G.J. Appleby-Thomas, and G.S. Collins, *Journal of Physics: Conference Series*, 2014. **500**: p. 112047.
8. Bourne, N.K., et al., [Measurement Science and Technology](#), 1995. **6**: p. 1462.
9. Braithwaite, C.H., J.I. Perry, and N.E. Taylor, [AIP Conference Proceedings](#), 2018. **1979**(1): p. 110002.
10. Collins, A.L., et al., [International Journal of Impact Engineering](#), 2011. **38**(12): p. 951.
11. Addiss, J.W., et al., in *Rapid Penetration into Granular Media*, M. Iskander, S. Bless, and M. Omidvar, Editors. 2015, Elsevier: Oxford. p. 229.
12. Addiss, J.W., A. Collins, and W.G. Proud, [AIP Conference Proceedings](#), 2009. **1195**: p. 1313.
13. Møller, P.C.F. and D. Bonn, [EPL \(Europhysics Letters\)](#), 2007. **80**(3): p. 38002.